ATM mutations in major stereotyped subsets of chronic lymphocytic leukemia: enrichment in subset #2 is associated with markedly short telomeres

Veronika Navrkalova,[1,2,3] Emma Young,[3] Panagiotis Baliakas,[3] Lenka Radova,[2] Lesley-Ann Sutton,[3] Karla Plevova,[1,2] Larry Mansouri,[3] Viktor Ljungström,[3] Stavroula Ntoufa,[4] Zadie Davis,[5] Gunnar Juliusson,[6] Karin E. Smedby,[7] Chrysoula Belessi,[8] Panagiotis Panagiotidis,[9] Tasoula Touloumenidou,[4,10] Frederic Davi,[11] Anton W. Langerak,[12] Paolo Ghia,[13] Jonathan C. Strefford,[14] David Oscier,[5] Jiri Mayer,[1] Kostas Stamatopoulos,[4] Sarka Pospisilova,[1,2] Richard Rosenquist,[3] and Martin Trbusek[1]

[1]Department of Internal Medicine – Hematology and Oncology, University Hospital Brno and Faculty of Medicine, Masaryk University, Brno, Czech Republic; [2]Department of Molecular Medicine, CEITEC - Central European Institute of Technology, Masaryk University, Brno, Czech Republic; [3]Department of Immunology, Genetics and Pathology, Science for Life Laboratory, Uppsala University, Sweden; [4]Institute of Applied Biosciences, CERTH, Thessaloniki, Greece; [5]Department of Molecular Pathology, Royal Bournemouth Hospital, UK; [6]Department of Laboratory Medicine, Stem Cell Center, Hematology and Transplantation, Lund University, Sweden; [7]Department of Medicine Solna, Clinical Epidemiology Unit, Karolinska Institutet, Stockholm, Sweden; [8]Hematology Department, General Hospital of Nikea, Piraeus, Greece; [9]First Department of Propaedeutic Medicine, School of Medicine, University of Athens, Greece; [10]Hematology Department and HCT Unit, G. Papanicolaou Hospital, Thessaloniki, Greece; [11]Laboratory of Hematology, Hospital Pitie-Salpetriere and University Pierre and Marie Curie, Paris, France; [12]Department of Immunology, Erasmus MC, University Medical Center Rotterdam, the Netherlands; [13]Division of Experimental Oncology and Department of Onco-Hematology, IRCCS San Raffaele Scientific Institute, Milan, Italy; and [14]Cancer Sciences, Faculty of Medicine, University of Southampton, UK

Correspondence: m.trbusek@volny.cz
doi:10.3324/haematol.2016.142968

Supplementary methods

Patient material

This study included CLL patients assigned to one of eight major stereotyped subsets #1-8 (n=249) that form part of a large European multicenter cohort; this cohort consisted of Czech (n=85), Greek (n=69), Dutch (n=42), Swedish (n=25), French (n=15), British (n=12), and Italian (n=1) cases. The cohort consisted predominantly of patients with unmutated IGHV genes (76%; 188/249). Clinical and biological features of the patient cohort are summarized in Supplementary Table 1. The biological material used in this study included separated B-lymphocytes or peripheral blood mononuclear cells. The leukemic cell fraction was assessed by flow cytometry and exceeded 80% in all cases (median 92%).

ATM mutation analysis

The entire coding region (62 exons) and adjacent splicing sites of the *ATM* gene were investigated using targeted deep-sequencing approaches (n=237 samples) or Sanger sequencing (n=12 samples). Concerning the deep sequencing, one hundred and fifty-two samples were analyzed using Haloplex technology (Agilent Technologies, CA, USA) according to the manufacturer's protocol. In brief, probes targeting all coding exons were designed and paired-end sequencing was performed on the HiSeq2000 instrument (Illumina, CA, USA) rendering a mean depth of ~1500 reads. The following software was used to process the sequences: Cutadapt (v.0.9.3) to remove adapter sequences, Mosaik (v.2.1.33) to align reads to the hg19 reference genome, SNPmania (an in-house tool, Uppsala) for variant detection and Annovar for variant annotation. Eighty-five Czech samples were analyzed using an in-house multiplex PCR protocol (University Hospital Brno) for *ATM* amplicons, Nextera XT kit for library preparation and sequenced on MiSeq instrument (Illumina, CA, USA). The median coverage was ~4000 reads and data was analyzed by CLC Genomic Workbench and Annovar. A conservative variant allele frequency (VAF) cut-off of 10% was selected for both deep sequencing approaches to avoid false-positives[1].

Other molecular characterization of the cohort

Cytogenetic lesions 17p13 deletion, 11q22-23 deletion, trisomy 12 and 13q14 deletion were detected by interphase fluorescence *in situ* hybridization (I-FISH) using locus-specific probes according to the individual centers' protocols. I-FISH data were available for 198 of 249 patients (80%). Mutational screening of recurrently affected genes was performed by next-generation sequencing (NGS) or Sanger sequencing. This included targeted screening of *TP53*, *NOTCH1, SF3B1*, and *BIRC3* genes performed either in Uppsala or Brno laboratory (protocols and primers are available upon request).

Relative telomere length analysis

Telomere length (TL) was assessed by real-time quantitative PCR using β-globin (HBB) as a single-copy gene and Human Genomic DNA (Promega, USA) as a reference DNA. Genomic DNA was extracted from CLL cells following standard protocols and diluted to 20 ng/μl with TE buffer. Prior to TL analysis, DNA from the samples to be analyzed and from the reference human DNA were diluted to a final concentration of 1.75 ng/μl in a TE buffer containing 2.5 ng/μl *Escherichia coli* DNA (Sigma–Aldrich, USA). The diluted samples were then denatured at 95°C for 5 min and cooled at 4°C. The PCR master mixes for telomeres (TEL) and HBB were slightly different, however final concentration of 10 mM Tris–HCl (pH 8.0), 10 nM Rox (Thermo Scientific, MA, USA), 1× Maxima Sybr Green qPCR MM (Thermo Scientific, MA, USA) and 1% DMSO was the same for both mixes. Final concentrations specific to the telomere mix were 100nM primer Tel1, 900nM primer Tel2, and 2.5 mM DTT, while for the HBB mix final concentrations were 400nM for both the HBG3 and HBG4 primers, and 5 mM DTT. The volume of each reaction was 25 μl, containing 5 μl of DNA (total amount 8.8 ng). Cycling conditions for the telomere amplification comprised an initial denaturation step at 95°C for 10 min, and 25 cycles at 95°C for 15 s and 54°C for 1 min. The same denaturation step was used for the HBB amplification, but was then followed by 35 cycles at 95°C for 15 s and 56°C for 1 min. All samples were loaded in triplicates and run on the Stratagene Mx3005P instrument (Agilent Technologies,

Santa Clara, CA). Primer sequences for telomeric repeats and the single-copy β-globin (HBB) gene are available upon request.

Relative telomere length (RTL) was calculated using the $2^{-\Delta\Delta Ct}$ method which compared the telomere to the single copy gene (T/S) ratio between a sample and the reference DNA. T/S values were determined using the formula $2^{-\Delta Ct}$ where ΔCt indicates the difference between the average Ct value for telomeres and for the HBB gene. The reference DNA was also used to monitor the PCR efficiency that reached 115% for telomere and 110% for HBB amplification. The inter-assay variability was evaluated under the fixed threshold (0.5 for TEL and 0.3 for HBB) and coefficients of variation (CV) were calculated to be 4% and 2.23% for Ct TEL and HBB, respectively. The intra-assay variability was measured in seven replicates on one plate and deemed to be 2% and 0.6% for TEL and HBB, respectively. Specificity of the assay was confirmed by gel electrophoresis and melting curve analysis.

Statistical evaluation

The chi-square test (χ^2) was used to assess differences in mutations frequencies, the Mann-Whitney U test to compare telomere lengths amongst the various subgroups and the log-rank test enabled comparisons of survival curves. All analyses were performed using the free statistical software R[42]. Overall survival (OS) and time-to-first-treatment (TTFT) were measured from the date of diagnosis until last follow-up/death or date of initial treatment, respectively. The significance level was set at $p<0.05$.

References

1. Sutton LA, Ljungstrom V, Mansouri L, Young E, Cortese D, Navrkalova V et al., Targeted next-generation sequencing in chronic lymphocytic leukemia: a high-throughput yet tailored approach will facilitate implementation in a clinical setting. Haematologica. 2015;100(3):370-376.

Supplementary tables and figures

Table 1: Clinical and biological characteristics of CLL patients included in the study.

Parameter	**Subset cohort (n=249)**		
	Number	total N	Ratio
Age at diagnosis: median (range)	62 (35-85)	210	
Gender (M/F)	137/90	227	1.5 : 1
Clinical stage			
Rai 0	60	204	29%
Rai I, II	91		45%
Rai III, IV	53		26%
*Therapy status**			
Untreated	109	143	76%
Treated	34		24%
IGHV gene somatic hypermutation status			
Mutated	61	249	24%
Unmutated	188		76%
*Hierarchical FISH**			
17p-	11	198	6%
11q-	50		25%
tri12	16		8%
13q- sole	53		27%
Normal	68		34%
* at sampling time			

Table 2: Frequency of cytogenetic aberrations (not hierarchically) in individual subsets #1 to #8.

Aberration (n; %)	#1	#2	#3	#4	#5	#6	#7	#8
del 17p	3; 7%	0; 0%	2; 18%	0; 0%	0; 0%	1; 8%	4; 16%	1; 8%
del 11q	10; 23%	16; 22%	6; 55%	0; 0%	3; 33%	1; 8%	15; 60%	1; 8%
Tris 12	6; 14%	2; 3%	0; 0%	0; 0%	3; 33%	0; 0%	3; 12%	5; 42%
del 13q	10; 23%	37; 51%	4; 36%	5; 38%	4; 44%	3; 23%	14; 56%	2; 17%
Normal	17; 40%	23; 32%	4; 36%	8; 62%	0; 0%	8; 61%	2; 8%	5; 42%
Number of patients	43	72	11	13	9	13	25	12

Table 3: Detailed description of 61 *ATM* mutations identified in 47 CLL patients.

Patient	Subset	Nucleotide change	Amino acid change	Type	ATM domain	Reported previously	VAF (%)	11q- (%)
P1	1	c.7354C>G	p.Leu2452Val	ms-neu	FAT	no	49	0
P2	1	c.8933del	p.Thr2978fs	fs	p53 int.	no	15	0
		c.8180T>C	p.Val2727Ala	ms	PIK	MCL	47	
P3	1	c.9064dup	p.Glu3022fs	fs	no	no	47	ND
P4	1	c.9032T>A	p.Met3011Lys	ms	p53 int.	CLL	84	ND
P5	1	c.8672G>A	p.Gly2891Asp	ms	PIK, p53 int.	CLL, AT	41	ND
P6	1	c.1561_1562del	p.Glu522fs	fs	no	no	99	0
P7	1	c.7736G>C	p.Arg2579Thr	ms-neu	no	no	45	ND
		c.283C>T	p.Gln95*	ns	TAN	no	83	
P8	1	c.3382C>T	p.Gln1128*	ns	b-adaptin int.	AT, ESCC	28	ND
P9	1	c.748C>T	p.Arg250*	ns	no	AT, CC	43	ND
P10	2	c.3062T>A	p.Val1021Glu	ms	b-adaptin int.	no	14	0
P11	2	c.6116A>G	p.Glu2039Gly	ms	no	no	18	0
		c.6364_6375del	p.Thr2122_His2125del	if	FAT	no	11	
		c.7630del	p.Leu2544*	ns	no	no	33	

P12	2	c.875C>G	p.Pro292Arg	ms	no	no	90	97
		c.7375C>T	p.Arg2459Cys	ms	FAT	no	100	
P13	2	c.6820G>A	p.Ala2274Thr	ms	FAT	CLL, BC	86	83
P14	2	c.5944C>T	p.Gln1982*	ns	no	no	58	0
P15	2	c.8264A>C	p.Tyr2755Ser	ms	PIK	no	69	78
P16	2	c.6056A>G	p.Tyr2019Cys	ms	no	AT, MCL	33	ND
		c.1430A>G	p.Lys477Arg	ms-neu	no	no	10	
P17	2	c.2961T>G	p.Cys987Trp	ms	b-adaptin int.	no	44	0
		c.8786+1G>A	p.?	spl	p53 int.	no	36	
P18	2	c.3118A>G	p.Met1040Val	ms-neu	b-adaptin int.	TCL	51	0
P19	2	c.4907del	p.Gln1636fs	fs	no	no	52	61
		c.4909+1del	p.?	spl	no	no	52	
P20	2	c.8050C>T	p.Gln2684*	ns	no	no	13	47
P21	2	c.7435_7438del	p.Glu2479fs	fs	FAT	no	29	ND
		c.7440del	p.His2480fs	fs	FAT	no	29	
		c.6679C>T	p.Arg2227Cys	ms	FAT	CLL, AT, ACC	59	
P22	2	c.2476A>C	p.Ile826Leu	ms-neu	no	CLL	63	ND
P23	2	c.6975+2T>C	p.?	spl	FAT	no	11	0

		c.9022C>T	p.Arg3008Cys	ms	p53 int.	CLL, MCL, PLL	16	
P24	2	c.3574A>G	p.Lys1192Glu	ms	b-adaptin int.	no	17	0
P25	2	c.4420C>G	p.His1474Asp	ms	no	no	49	0
P26	2	c.8315del	p.Gly2772fs	fs	PIK	no	98	0
P27	2	c.2705dup	p.Phe903fs	fs	no	no	11	ND
P28	2	c.3237del	p.Asp1080fs	fs	b-adaptin int.	no	78	ND
P29	2	c.8310C>G	p.Cys2770Trp	ms	PIK	no	42	ND
P30	2	c.8249T>C	p.Leu2750Ser	ms	PIK	CLL	NP	76
P31	3	c.8368A>T	p.Arg2790*	ns	PIK	no	45	93
P32	3	c.6185C>T	p.Ala2062Val	ms-neu	no	no	60	87
P33	4	c.2554C>T	p.Gln852*	ns	no	CLL	30	0
P34	5	c.4993_4996del	p.Glu1666fs	fs	no	no	67	77
P35	5	c.7327C>G	p.Arg2443Gly	ms	FAT	CLL, AT	NP	84
P36	6	c.7463G>A	p.Cys2488Tyr	ms	FAT	CLL	38	0
		c.7878_7882del	p.Ile2629fs	fs	no	no	25	
P37	6	c.869A>T	p.His290Leu	ms	no	no	25	ND
P38	6	c.3101dup	p.Tyr1034fs	fs	b-adaptin int.	no	41	0
		c.5496+2T>G	p.?	spl	no	no	43	

P39	6	c.7515+1G>A	p.?	spl	no	no	NP	86
P40	7	c.7280T>C	p.Leu2427Pro	ms	FAT	CLL, CRC	91	94
P41	7	c.3250C>T	p.Gln1084*	ns	b-adaptin int.	CLL	46	99
P42	7	c.3075T>G	p.Phe1025Leu	ms	b-adaptin int.	no	95	93
P43	7	c.6101G>C	p.Arg2034Pro	ms	no	no	100	95
P44	7	c.4804G>T	p.Val1602Phe	ms-neu	no	no	88	93
P45	7	c.2720_2723del	p.Cys907fs	fs	no	CLL	NP	93
P46	7	c.6375insT	p.Glu2126fs	fs	FAT	CLL	NP	84
P47	8	c.3077+2T>A	p.?	spl	b-adaptin int.	no	46	0
		c.7456C>T	p.Arg2486*	ns	FAT	AT, CC	47	

Legend: ACC-Adenoid Cystic Carcinoma, AT-Ataxia telangiectasia, BC-Breast Cancer, CC-Colon Cancer, CLL-Chronic Lymphocytic Leukemia, CRC-Colorectal Cancer, ESCC-Esophageal Squamous Cell Carcinoma, ND-Not Determined, NP- Not Provided, ms: missense; ms-neu: missense with presumably neutral impact; ns: nonsense; fs: frameshift; spl: affecting splicing site; PLL-Prolymphocytic Leukemia, TCL-T-Cell Leukemia, VAF-Variant Allele Frequency

Table 4: Number of samples with particular genetic defect in individual subsets tested for RTL.

Genetic category	#1	#2	#3	#4	#5	#6	#7	#8	Total
Def-*TP53*	16	6	1	1	0	3	5	2	34
Def-*ATM*	2	8	2	0	1	2	5	1	21
Sole 11q-	6	6	3	0	1	0	6	1	23
Sole *ATM*-mut	1	5	0	1	0	0	0	0	7
WT	19	39	3	11	5	6	7	8	98
Unknown	15	4	1	0	3	1	4	2	30
Total	59	68	10	13	10	12	27	14	213

Figure 1: Mutation distribution in individual subsets #1 to #8: A) *ATM*, B) *TP53*, C) *SF3B1*, D) *NOTCH1* and E) *BIRC3* genes (red: mutated, gray: unmutated; mutation frequency is given above the bars). Statistical significances between individual subsets are shown in the tables below the figures.

A) *ATM* mutations

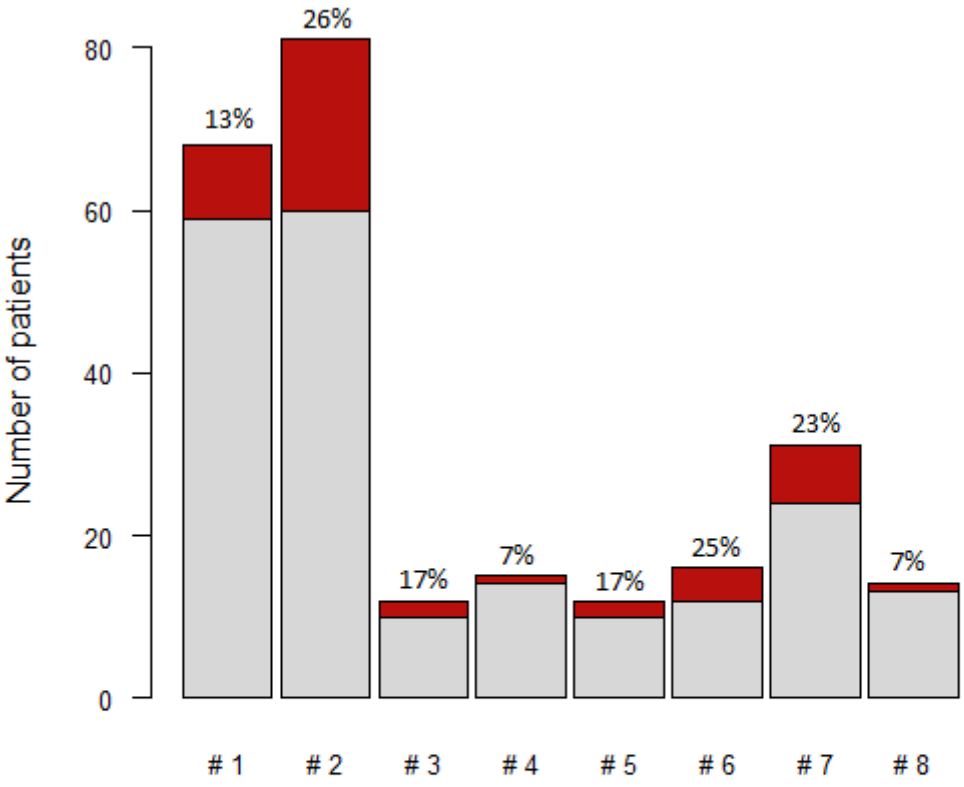

Chi-square test:	#2	#3	#4	#5	#6	#7	#8
#1	0,09	1,00	0,79	1,00	0,43	0,38	0,85
#2		0,74	0,20	0,74	1,00	0,90	0,23
#3			0,84	1,00	0,95	0,99	0,89
#4				0,84	0,37	0,36	1,00
#5					0,95	0,99	0,89
#6						1,00	0,41
#7							0,40

B) *TP53* mutations

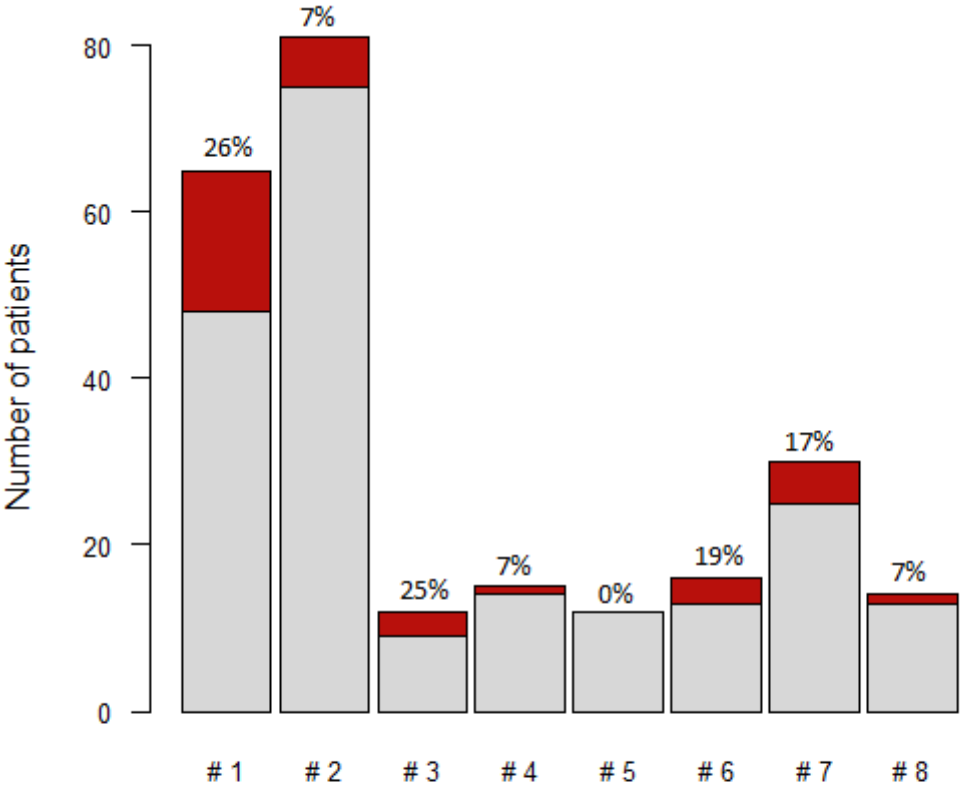

Chi-square test:	#2	#3	#4	#5	#6	#7	#8
#1	0,001	1,00	0,20	0,10	0,77	0,45	0,24
#2		0,16	1,00	0,73	0,34	0,27	1,00
#3			0,43	0,22	1,00	0,85	0,48
#4				1,00	0,64	0,64	1,00
#5					0,33	0,33	1,00
#6						1,00	0,69
#7							0,70

C) *SF3B1* mutations

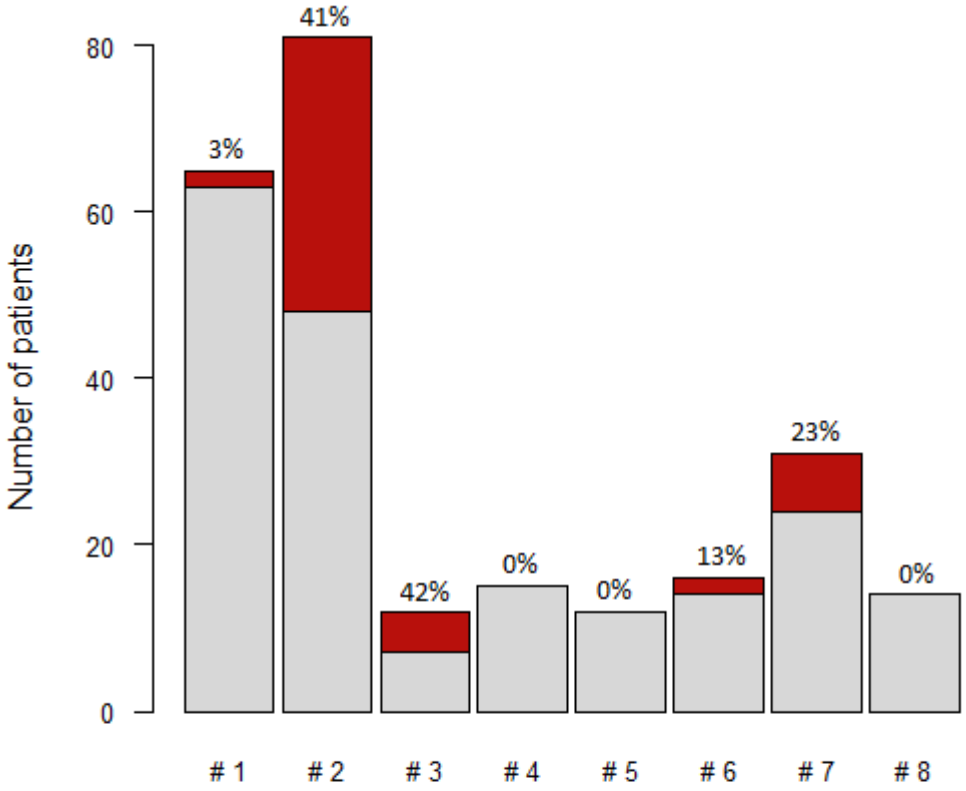

Chi-square test:	#2	#3	#4	#5	#6	#7	#8
#1	0,001	0,001	1,00	1,00	0,36	0,01	1,00
#2		1,00	0,01	0,02	0,06	0,12	0,01
#3			0,02	0,04	0,19	0,38	0,03
#4				NA	0,49	0,12	NA
#5					0,60	0,18	NA
#6						0,66	0,52
#7							0,14

D) *NOTCH1* mutations

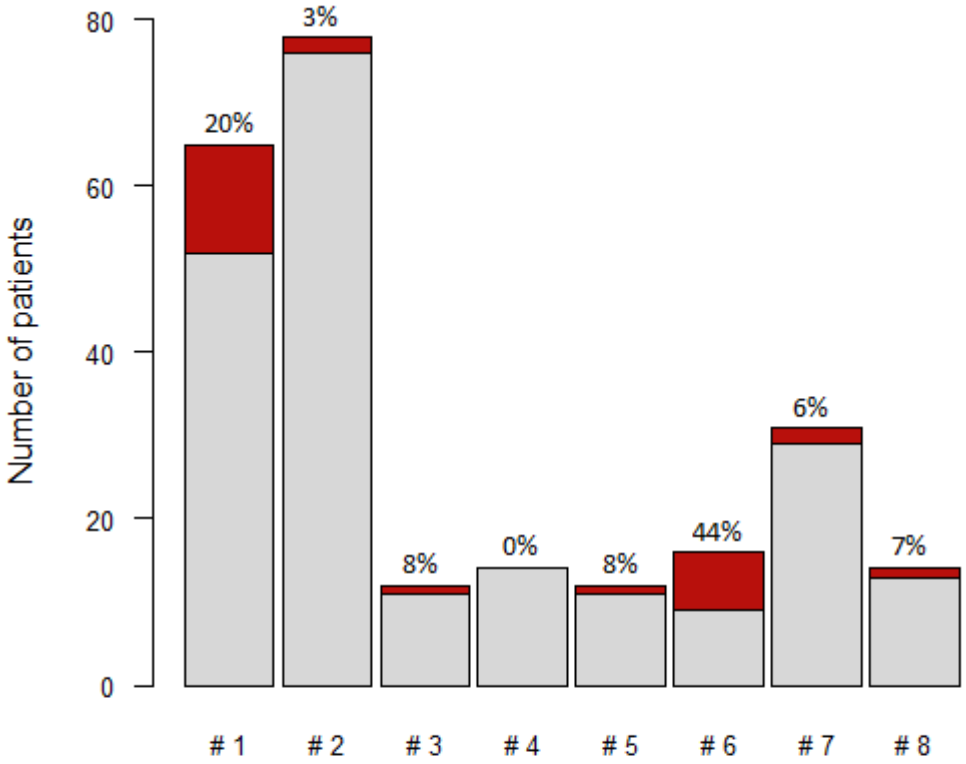

Chi-square test:	#2	#3	#4	#5	#6	#7	#8
#1	0,001	0,58	0,15	0,58	0,10	0,16	0,45
#2		0,86	1,00	0,86	0,001	0,68	0,94
#3			0,94	1,00	0,10	1,00	1,00
#4				0,94	0,02	0,85	1,00
#5					0,10	1,00	1,00
#6						0,01	0,06
#7							1,00

E) *BIRC3* mutations

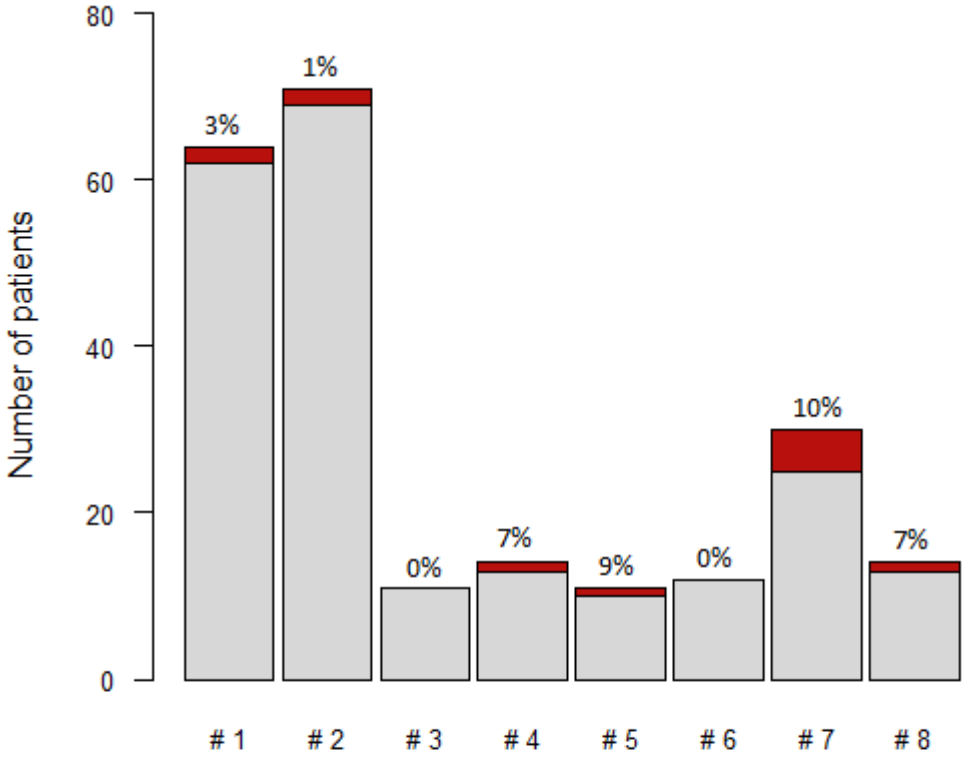

Chi-square test:	#2	#3	#4	#5	#6	#7	#8
#1	1,00	1,00	1,00	0,92	1,00	0,06	1,00
#2		1,00	0,99	0,87	1,00	0,04	0,99
#3			1,00	1,00	NA	0,36	1,00
#4				1,00	1,00	0,70	1,00
#5					0,96	0,91	1,00
#6						0,33	1,00
#7							0,70

Figure 2: Relative telomere length in major stereotyped subsets #1 to #8. Statistical significances between individual subsets are shown in the table below the figure.

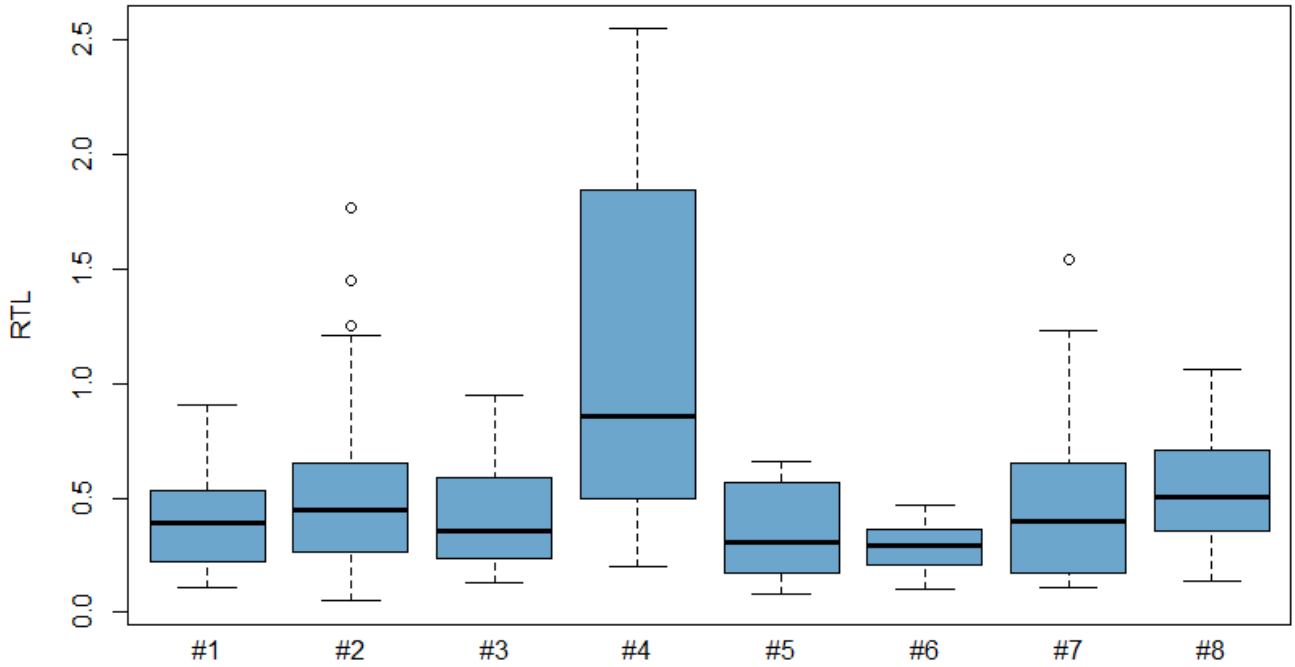

Mann-Whitney test:	#2	#3	#4	#5	#6	#7	#8
#1	0,13	0,95	0,001	0,65	0,12	0,85	0,10
#2		0,40	0,002	0,19	0,02	0,47	0,45
#3			0,01	0,71	0,37	0,76	0,24
#4				0,003	0,001	0,003	0,04
#5					0,49	0,46	0,12
#6						0,20	0,01
#7							0,27

Figure 3: Relative telomere length in M-CLL and U-CLL patients in subset #2 (medians 0.45 and 0.37, respectively; p=0.51).

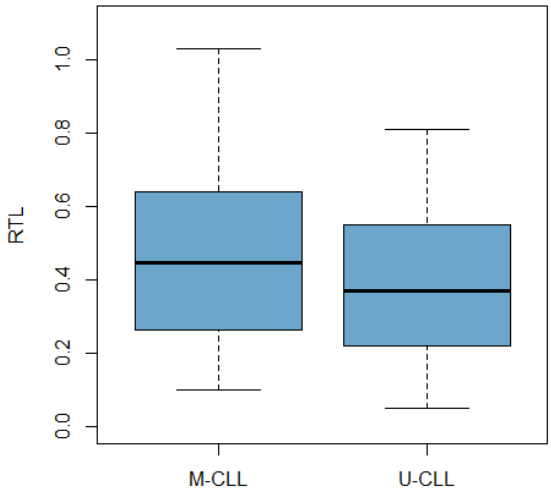

Figure 4: Relative telomere length according to genetic defect presence in subset #2 U-CLL cases. Statistically significant difference is marked in the graph.

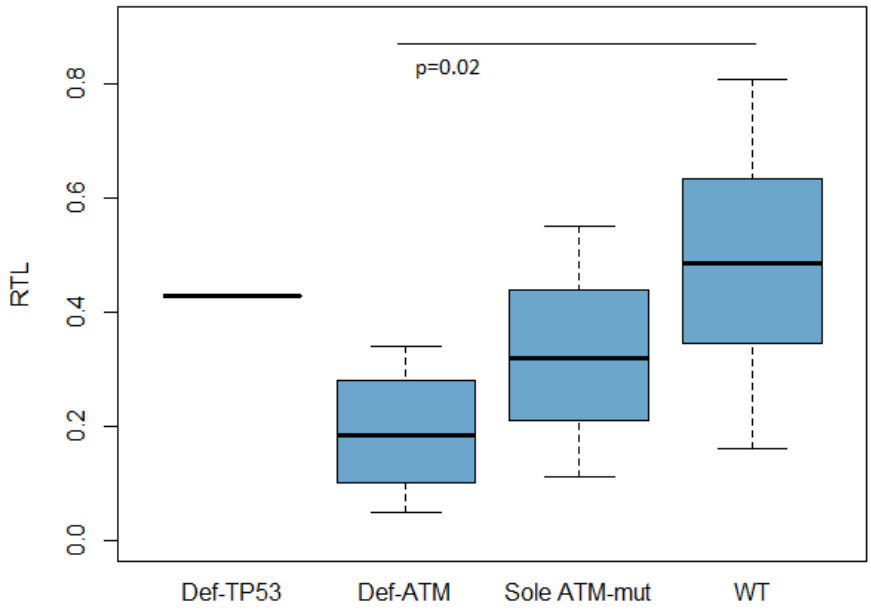

Figure 5: Overall survival of subset #2 patients considering the presence of *TP53* and *ATM* defects hierarchically. Borderline statistical differences between genetic groups and WT are marked in the graph with corresponding colors.